

5th Australasian Congress on Applied Mechanics, ACAM 2007
10-12 December 2007, Brisbane, Australia

Stress and fracture analysis of circular arc blends for repair of cracked metallic components

M Burchill and M Heller

Air Vehicles Division, Defence Science and Technology Organisation, Melbourne, Victoria

Abstract: This paper presents compact functions for peak stresses and stress decay distributions due to circular arc blend repairs, on circular holes in uniaxially loaded plates. Key geometric parameters are varied, focusing on relatively shallow blends, consistent with the in-service repair of fatigue cracking in ageing airframes. The highly accurate stress results are obtained using adaptive p-version finite element analyses. In the 2D cases, both single and double sided repairs are considered, where the blend consists of either a single or multi-arcs. For the 3D analyses, the focus is on blends to repair corner cracks at the hole edge. It is found that in all cases, the peak stress can be significantly reduced by maximising the ratio of blend radius to hole radius, thereby lowering the possibility of re-cracking. The multi-arc case offers the greatest stress reduction. The stress decay functions presented can be used to obtain stress intensity factors for the fatigue analysis of cracks which may re-initiate at the blends.

Keywords: stress concentration, stress intensity factor, crack repair, finite element analysis, fatigue life extension.

1 Introduction

One common method for repairing cracked metallic airframe components in aging aircraft is to remove the cracks using circular arc “blends”. This has the advantage of being a relatively simple approach which does not require the use of complex tooling, or the replacement of the component (which may be expensive or impractical). Such blends are applicable to maintaining ageing aircraft as well as the repair of fatigue test articles. Ideally after blending, the resultant stress concentration should not be significantly greater than the initial uncracked configuration (to delay the onset of further cracking). Key geometric parameters which affect the stress concentration are the blend depth and blend radius.

For successful application, the peak stresses due to the blend must to be accurately quantified. For circular or optimised blends to flat surfaces, stress peaks are fairly well defined [1,2,3]. Also some simple guidelines are given by the airframe manufacturers, regarding blend design and the associated stress increases. However, it is more common for cracks to occur on curved surfaces, at locations such as holes and section transitions. For these cases only limited data on stress concentration exists for shallow blends. For example some published graphical results, based on semi-analytical methods for 2D cases are given in [4,5,6]. However, compact accurate functions for stress concentration factors, for a range of the key parameters are not available which could be used by analysts. Furthermore, for 3D geometries no results have currently been found in the literature. Hence it is unclear, for either 2D or 3D cases, what is the best choice of aspect ratio and or relative radii for a given repair depth. Also, for structural fatigue life management based on the periodic inspection of components, the stress intensity factor [7], or the stress decay along the prospective crack path, is of key importance. This is because after blending, the rate of crack growth needs to be determined for possible subsequent cracking. Such stress decay information is currently not available in an accurate or compact form.

Hence in the present paper a thorough parametric investigation is undertaken to determine peak stresses and stress decay for circular arc blends to curved surfaces such as circular holes in loaded plates. To allow efficient calculation of the stress quantities, finite element analysis is undertaken using adaptive p-version elements. Initially the geometry definition for the range of cases considered is presented in Section 2. Sections 3 and 4 then give the results of the parametric study and compact functions for the 2D stress peaks and local stress decay respectively. In Section 5 some 3D results for stress peaks are given. Following this, Section 6 gives examples where the approach can be used, including a successful application to a full scale fatigue test article. Key results are presented in non-dimensional form, as compact functions, to have wide utility.

2 Numerical method

2.1 Blended hole geometry

The 2D geometry under consideration is given in Figure 1. Here Figures 1a and 1b show a large uniaxially loaded plate containing a circular hole with either two or one circular arc blends respectively. The remote uniform stress is S , the plate width and height is $2W$, the initial hole radius is r_1 , the blend radius is r_2 and the blend depth is given by d . Figure 1c shows the geometry where the blend is multi-arc. That is, three arcs where the centre arc again is defined as r_2 , over the angular range $\pm \alpha$, while the two transition arcs are r_3 . The key reasoning for this case is that it is the simplest configuration which allows the blend radius, r_2 to be greater than r_1 at the location of maximum stress. Further discussion of this issue is given in Section 3.3, where a double sided multi-arc case is also considered. It is noted, that as r_2/r_1 and α increase the double-sided multi-arc can tend towards an optimal hole shape; but this issue is beyond the scope of the present paper. Note that in all 2D cases, the blends are symmetric about the x - axis and situated, at the most probable crack location, where the stresses are greatest. The range of geometries considered focuses on relatively shallow blends, as commonly seen in aircraft service, so that; $0.05 \leq d/r_1 \leq 0.50$, $0.7 \leq r_2/r_1 \leq 3.0$, and $0.25 \leq r_3/r_1 \leq 0.50$. The 3D geometry is shown in Figure 2, where the blend is a partial 45° chamfer at one edge of the hole. This is a typical location for cracking and the blend is essentially an extension of the 2D case (seen in Figure 1c) to 3D. Note however in 3D we fix r_2 , so that $r_2 = r_1 + d$. The reason for this choice is discussed further in Section 6. The parameter range considered is consistent with the 2D cases, however we add for 3D, $0.2 \leq t/r_1 \leq 2.0$. For all analysis cases Young's modulus is 70,000MPa and Poisson's ratio is 0.3.

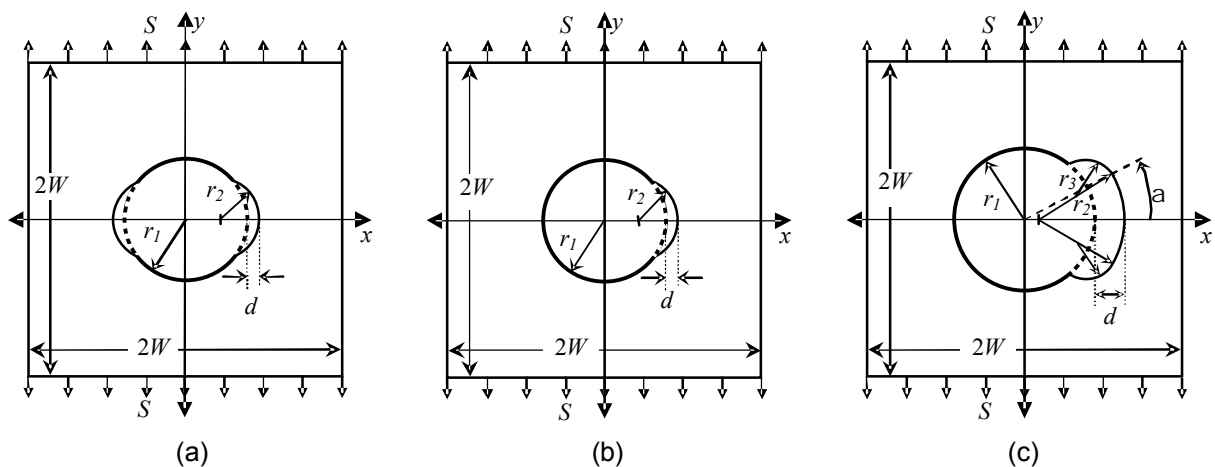


Figure 1. Geometry and notation for large 2D plates with a circular hole and circular arc repairs: (a) one circular arc blend on both sides of hole, (b) one circular arc blend on one side of hole and (c) multi-arc blend on one side of hole.

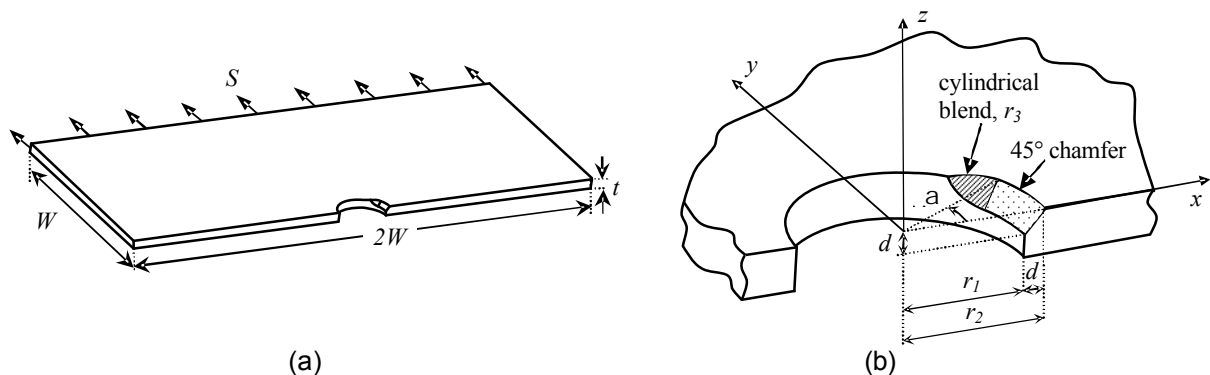


Figure 2. Geometry for hole in a large 3D plate with multi-arc blend on one side of hole: (a) plate dimensions and loading, with only $\frac{1}{2}$ section shown, and (b) local details around blend.

2.2 Finite element analysis method

The FE stress analysis code StressCheck[®] was used for all analyses. This code runs on a standard PC and has some useful features for the present work. Firstly the use of variable order polynomial elements (p-version elements) means that a relative coarse geometric mesh can be used, allowing for quick mesh creation but with a high level of accuracy. Secondly, multiple FE models can be created and the results processed automatically, based on separate parameters for geometry, loading or material conditions. This is done via a second program such as Excel using Visual Basic (which was done here). Typically, the 2D FE models have less than 200 quadrilateral elements. However, as higher order p-version elements (6 to 8 order) are used, the degrees-of-freedom (DOF) of the stiffness matrix can be as high as 10,000 in 2D. The 3D geometry requires many more elements, with approximately 2000 tetrahedral 8th order elements being used, having up to 1,000,000 DOF. Symmetry conditions are used as appropriate in the analyses. An example of a typical 2D mesh and contours of maximum principle stress are shown in Figure 3a. This is for the case of a double sided circular arc blend, where $S = 100\text{MPa}$, $r_1 = 10\text{mm}$, $r_2/r_1 = 0.8$, $W = 20r_1$ and $d/r_1 = 0.2$. A typical 3D example is shown in Figure 3b for a single multi-arc blend, where $S = 100\text{MPa}$, $r_1 = 10\text{mm}$, $W = 20r_1$ and $d/t = d/r_1 = 0.5$, $a = 30^\circ$ and $r_3/r_1 = 0.5$.

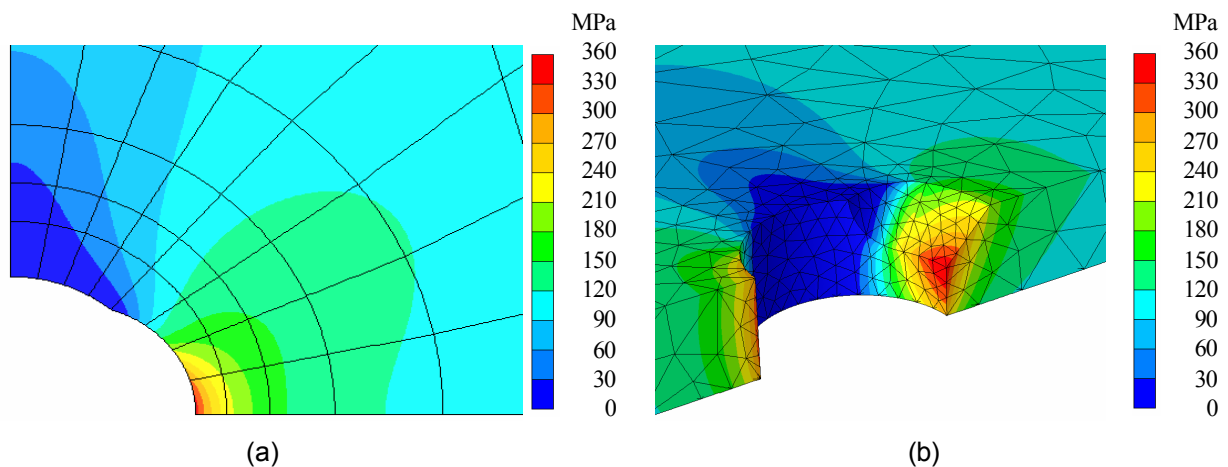


Figure 3. Local mesh and stress distributions for typical p-version FE models: (a) 2D, and (b) 3D.

The accuracy of the FE model can be quickly assessed for a particular case by plotting convergence of the maximum normalised stress ($K_t = S_{\text{peak}}/S$) and the percentage error in the potential energy (PE) estimate. This error estimate is based on the PE difference between successive p-version element order analyses. This is shown in Figures 4a and 4b, where each dot refers to a particular p-version element order, ranging from 1 for low DOF's and 8 for high DOF's.

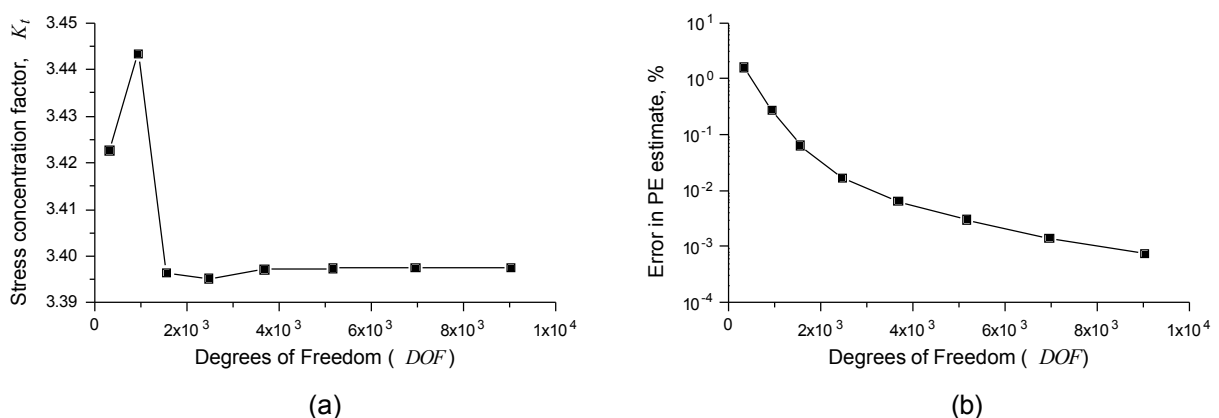


Figure 4. Typical results of a convergence study for 2D case: (a) stress concentration factor, and (b) error in the potential energy (PE) estimate.

3 Peak stresses for two dimensional cases

3.1 Single circular arc blend $r_2 < r_1$ – one or both sides of hole

Results of the parametric study for this case are presented as a function of d/r_2 and r_2/r_1 in Figure 5. As expected K_t reduces as r_2/r_1 is increased and d/r_1 is reduced. These results agree very well with limited published solutions [4,5,6]. An expression for K_t can be determined using linear regression, as:

$$K_t = m \frac{d}{r_2} + c \quad \text{where, } m = m_1 \frac{r_1}{r_2} + c_1 \quad \text{and} \quad c = m_2 \frac{r_1}{r_2} + c_2 \quad (1)$$

This gives:
$$K_t = 0.440n \frac{d}{r_2} - 1.300 \frac{r_2}{r_1} + 4.340 \quad \text{where } n \text{ is the number of blends, (i.e. 1 or 2)} \quad (2)$$

Use of (1) or (2) gives K_t values to within 1% of the initial FEA results, in the range: $0.05 \leq d/r_1 \leq 0.50$ and $0.7 \leq r_2/r_1 \leq 1.0$. As expected the lowest K_t as a function of d/r_1 is given by:

$$K_t = 3.040 + 0.440n \frac{d}{r_2} \quad \text{when } r_2 = r_1 \quad (3)$$

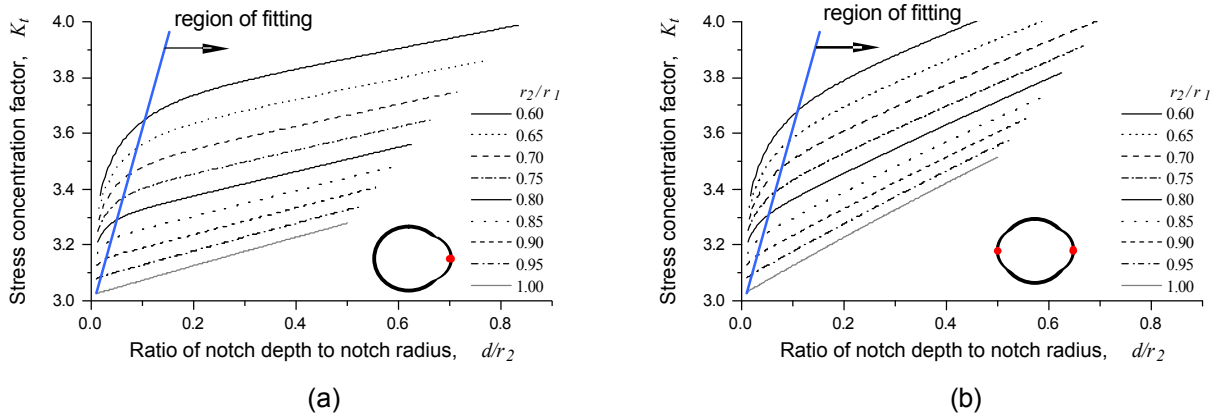


Figure 5. K_t variation for circular hole with single circular arc blend: (a) one side, and (b) on both sides.

3.3 Multi-arc blend $r_2 > r_1$ – one or both sides of hole

From the result trends in the proceeding section, it is clear that stresses will be further reduced when $r_2 > r_1$. To achieve $r_2 > r_1$ an additional arc, r_3 , is required to provide a closed hole shape, as shown in Figure 1c. From the parametric study undertaken for this case, where we fix $r_3/r_1=0.5$, the values of r_2/r_1 can be found for each a , that yield the minimum K_t in the blend. These results are summarised in Figures 6a and 6b below for the one sided case.

For this one sided case we can again use linear regression to define the conditions for minimum principle stress, σ_1 in the blend as:

$$\frac{S_1}{S} = 3.479 - 0.155 \frac{d}{r_1} - 1.814a, \quad \text{when } r_2 = 3.064ad - 0.188d + 3.485ar_1 \quad (4)$$

(Note the overall peak stress is typically located on the un-blended side of the hole, if $a > 20^\circ$ and $r_2 > 1.05r_1$). For the two sided case (not plotted) the expression for minimum blend stress or K_t is similarly given as:

$$K_t = 3.600 - 0.492a \frac{d}{r_1} + 0.335 \frac{d}{r_1} - 1.096a, \quad \text{when } r_2 = 2.571ad + 1.035ar_1 + 0.7602 \quad (5)$$

Both (4) and (5) apply in the range $20^\circ \leq a \leq 35^\circ$, $0.05 \leq d/r_1 \leq 0.5$ and $1.35 \leq r_2/r_1 \leq 3.0$, where a is given in radians.

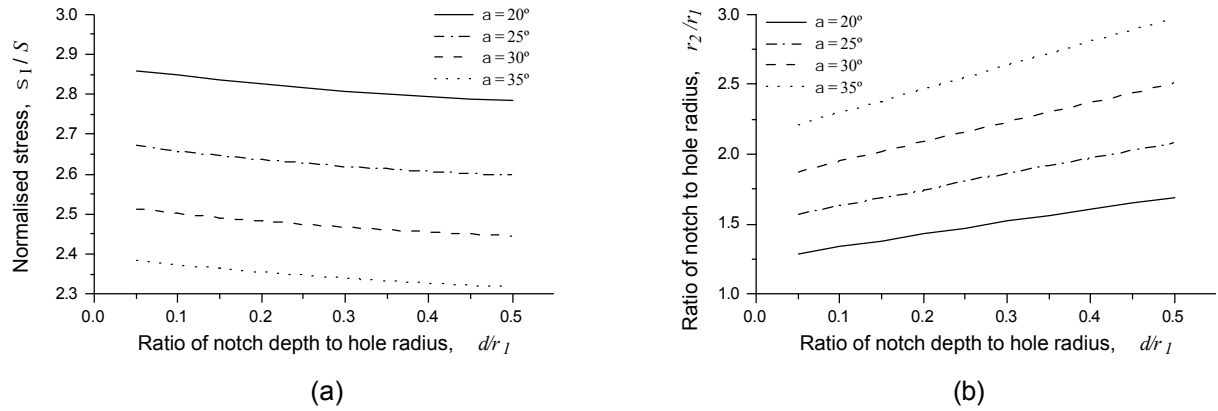


Figure 6. Minimum K_t results for single sided multi-arc blend on a hole with $r_3/r_1 = 0.5$: (a) effect of relative blend depth d/r_1 , and (b) required ratio of r_2/r_1 .

It is noted that for the one sided case the lowest possible K_t is approximately 2.32, when $a = 35^\circ$, $r_2/r_1 = 2.8$, and $d/r_1 = 0.5$. For the two sided case, when $a = 35^\circ$, the lowest possible K_t is approximately 2.72 regardless of d/r_1 . Also for both these cases, K_t is less than for the original unblended hole. From the full parametric results (not presented here) it was found, that for the case $r_2 = r_1$, the K_t values for the multi-arc (Section 3.3) and the single arc cases (Section 3.2) are equivalent (less than 0.5% difference).

4 Stress decay and stress intensity factors for two dimensional cases

4.1 Stress decay

Typical stress decay results along the x -axis are given in Figure 7 below for the single arc cases, for blends on one or both hole sides. For this particular example a range of blend depths $0.05 \leq d/r_1 \leq 0.50$ are considered, but we fix $r_2/r_1 = 0.85$. To initially collapse the data, the normalising functions used are:

$$\tilde{S} = \frac{3s}{S_{peak}} \quad \text{and} \quad \tilde{x} = (r_2 - r_1) + r_2(x - d) \quad (6)$$

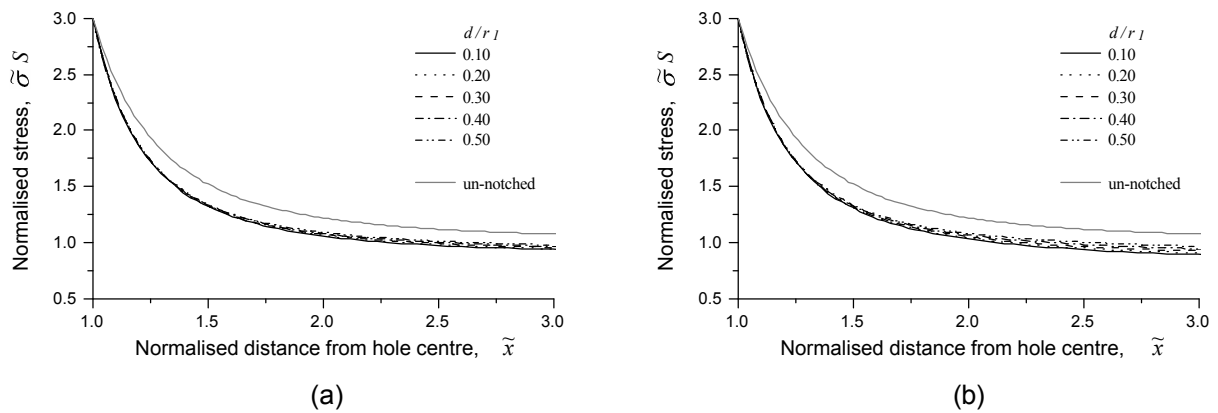


Figure 7. Normalised results for stress decay along the prospective crack path ($y = 0$) for a single arc blended hole with $r_2/r_1 = 0.85$: (a) blend on one side, and (b) blend on both sides.

Also plotted on the above figures is the analytical solution for an un-blended hole, where the stresses are given in [8], along the x -axis

$$s = \frac{S}{2} \left[2 + \frac{r_1^2}{x^2} + \frac{3r_1^4}{x^4} \right] \quad (7)$$

It is clearly seen from Figure 7 that with the normalisation, (5) the blended hole stress decay and that of the un-blended hole are similar. Hence a modified version of the un-blended hole stress decay is proposed to fit to the FEA data for all cases considered, as:

$$\tilde{s} = \frac{3}{2s_{peak}} \left[2 + \frac{r_2^2}{(a\tilde{x} + b)^2} + \frac{3r_2^4}{(a\tilde{x} + b)^4} \right] \quad (8)$$

The coefficients a and b were solved for (as a linear function of d and r_2) by using a non-linear curve fitting tool in the program Origin[®], for a range of geometries. The coefficients a and b are constrained such that $\tilde{s} = 3$ when $x = \tilde{x} = 1$, to ensure that the best fit is achieved at this peak stress location. For the single arc blend this leads to:

$$a = (0.1736d - 0.4934)r_2 - 0.4143d + 1.4742, \quad \text{and} \quad b = (-0.2458d + 1.6097)r_2 + 0.4211d - 1.5958 \quad (9)$$

while for the single arc blend on both sides, the coefficients are:

$$a = (0.2613d - 0.5147)r_2 - 0.6663d + 1.4873, \quad \text{and} \quad b = (-0.3879d + 1.6241)r_2 + 0.6770d - 1.6039 \quad (10)$$

The fitting of (8-10) is accurate for $r_1 \leq x \leq 3r_1$ to within 1% for blended holes where $0.05 \leq d/r_1 \leq 0.20$ and $0.85 \leq r_2/r_1 \leq 1.00$, and to within 2.5% for the extended range $0.05 \leq d/r_1 \leq 0.50$ and $0.75 \leq r_2/r_1 \leq 1.00$

4.2 Stress intensity factors – single circular arc blend case

For fracture or fatigue analysis of these repairs, we need to consider potential cracking (i.e. for after the repair is undertaken) along x -axis. The local geometry is as shown in Figure 8a. For this example we consider a through crack of length l (however the approach here is also applicable to partial thickness 3D cracks). First we recap that for an edge crack in a large rectangular plate, of length l , the stress intensity factor is given in [7] as:

$$K_I = S\sqrt{\rho}lb_e \quad (11)$$

where $b_e = 1.12$; this is the 2D edge crack correction factor. For the blend repair configuration, we can use (11), by replacing S with the local stress distribution s of the uncracked body, as given in (8), to define the stress intensity factor as:

$$K_I = s\sqrt{\rho}lb_e \quad (12)$$

where $l = x - r_1 - d$, and from (6) $\tilde{x} = (r_2 - r_1) + r_2(l + r_1)$ (13)

As an independent check, separate FEA analysis were undertaken of a single sided blended hole with $r_2/r_1 = 0.85$ and $d/r_1 = 0.25$, where the crack was explicitly modeled. The local detail of such a typical mesh is shown in Figure 8b. The analysis results are given in Figure 8c, where we compare values of the total geometry factor b_T , given by:

$$b_T = K_I / S\sqrt{\rho}l \quad (14)$$

It can be seen that the stress intensity factors from the FEA with the crack explicitly modelled are well predicted (less than 3% difference), directly from the equations of stress decay for the uncracked body (12) and (14).

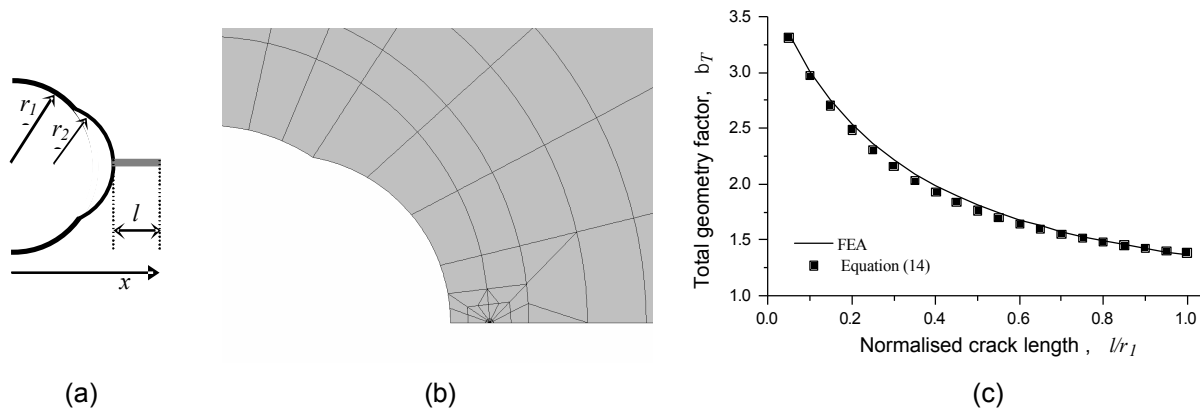


Figure 8. Analysis of stress intensity factors for a cracked single arc blended hole: (a) geometry for potential re-cracking at blend, (b) local FEA mesh with crack, with, $r_2/r_1 = 0.85$, $d/r_1 = 0.25$, and (c) comparison of b_T predictions for the uncracked body stress decay and FEA containing crack.

5 Peak stresses for three dimensional cases : multi-arc on one side

For most practical 3D cases it is desirable to have a blend geometry which is easy to implement with simple tools and gives a good stress reduction. Hence based on the proceeding results, such a repair geometry for a 2D multi-arc blend, is $r_2 \geq r_1$, $r_3 = 0.5r_1$ and $a = 35^\circ$. For 3D this approximately translates to the geometry shown previously in Figures 2b and 3b, where $r_2 = r_1 + d$. Hence a parametric study was undertaken for such a one sided repair, where the relative blend depth, d and plate thickness, t was varied. Results of the relative increase in K_t are given in Figure 9. As expected K_t increases with increasing d/t and t/r_1 It should be noted that the K_t values quoted here refer to the peak stress in the hole bore which includes the blend region. For very shallow blends, the peak stress is typically located near the centre of the plate, not in the blend region. As d/t increases and t/r_1 decreases, the peak stress location moves to the blend region.

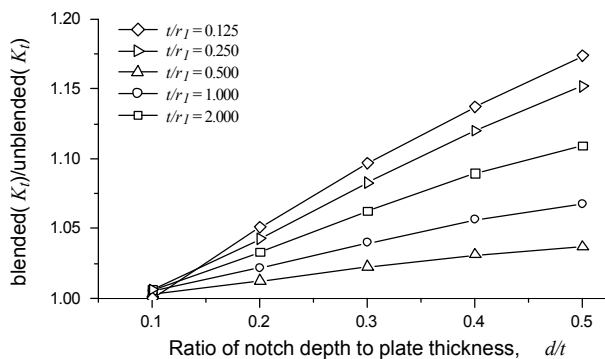


Figure 9. Stress Concentration increase for a range of partial chamfer blends where $\alpha = 35^\circ$, $r_3 = 0.5r_1$.

6 Practical applications

Recently the approach given in this paper has been applied to a number of practical 3D applications, including full scale wing fatigue test articles [9,10] and fleet aircraft [11]. For example cracking of an F-111 inboard pivot pylon hole in the upper skin, during a full scale fatigue test was repaired with the aim of minimising the K_t after the repair, [9]. This was a crucial fatigue test undertaken to determine the economic life of F-111 wings, and it was important to avoid re-cracking of the blend. The location of cracking on the aft side of the hole is shown in Figure 10a and Figure 10b. Here three cracks are seen; where the largest had a length of 0.12". A multi-arc repair was analysed and undertaken with the parameters, $d = 0.15"$, $r_1 = 3.875"$, $t = 0.68"$, $r_3 = 0.5r_1$, and $a \geq 35^\circ$. The stress increase as compared to the initial uncracked case was less than 5%. The complete repair is shown in Figure 10c. It was able to be undertaken rapidly, and the wing test was successfully run to completion with no further cracking at this location. It is noted that cracking also occurred on the other (forward) side of the hole, where a crack of 0.278" was similarly removed.

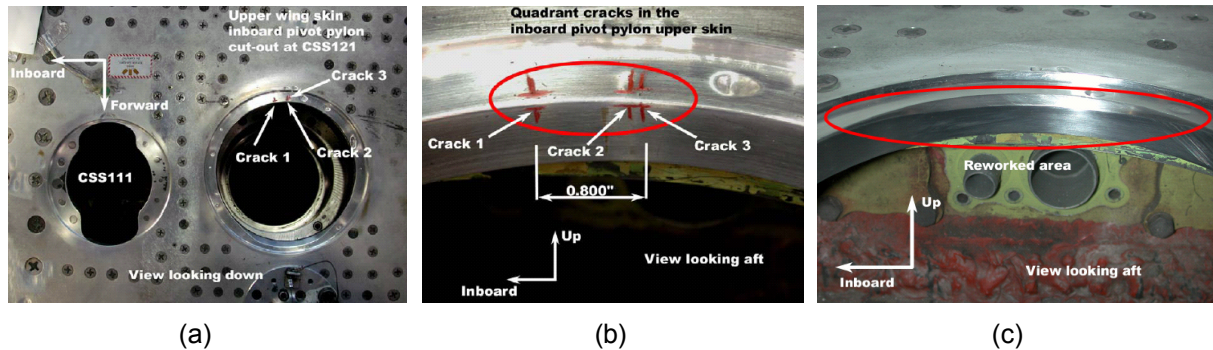


Figure 10. Repair blend on the F-111 wing test article, at the inboard pivot pylon upper hole: (a) upper wing skin near hole, (b) location of three quadrant cracks at hole, (c) completed multi-arc blend repair.

Apart from circular holes, the results in the present paper can be used to obtain a very good estimate for the relative stress increase on general curved surfaces due to a local blend. For example geometries such as: (i) non-circular holes and optimised holes, and (ii) local section transitions. To do this, the local radius of curvature at the crack location would be substituted in place of r_1 in equations (2) or (4) or (5).

7 Conclusions and recommendations

Accurate and compact functions (2D cases) are given for peak stresses and stress decay distributions due to circular arc blend repairs, on circular holes in uniaxially loaded plates. The results are relevant to the analysis of in-service repair of fatigue cracking in ageing airframes. Both single circular arc and multi-arc cases are considered. Single arc results have not previously been available in a convenient form, while the multi-arc is to an extent a new proposal. In all cases, the peak stress can be reduced by maximising the ratio of blend radius to hole radius, thereby lowering the possibility of re-cracking. The multi-arc case offers the greatest stress reduction, as it allows the local radius to be maximised, so that the stress concentration factor can be significantly less than the initial circular hole, (analogous to optimising the part of the hole shape). The stress decay functions given can be used to obtain stress intensity factors for the analysis of potential re-cracking at the blend. The benefits of the approach are demonstrated in a practical example, and suggestions for applications apart from circular holes are given. Follow-on work is proposed to fully define the 3D stress equations.

References

- [1] W. D. Pilkey. *Peterson's stress concentration factors*. John Wiley & Sons inc. 1997.
- [2] M Burchill, M Heller. Optimal notch shapes for loaded plates. *Journal of Strain Analysis for Engineering Design*. 39(1), pp.99-116. 2004.
- [3] R Wescott, B. Semple, M. Heller. Stress analysis of near optimal surface notches in 3D plates. *Transactions of the ASME: Journal of Mechanical Design*. 127, pp 1173-1182.
- [4] L H Mitchell. Stress-concentration factors at doubly-symmetric hole. *The Aeronautical Quarterly*, 1966, 17, 177-186.
- [5] K Miyao. Stresses in a plate containing a circular hole with a notch. *Bulletin of the JSME*, 1970, 13 (58), 483-490.
- [6] H Nisitani, N-A Noda. Stress concentration of a strip with double edged notches under tension or in-plane bending. *Engineering Fracture Mechanics*, 1986. 23(6), 1051-1065.
- [7] D. Broek, *The practical use of fracture mechanics*. Kluwer Academic Publishers, 1988.
- [8] S P Timoshenko, J N Goodier. *Theory of elasticity* 3rd edition, 1982, McGraw Hill.
- [9] T V Blaricum, M Burchill, A Tatangelo. Repair Disposition of cracking at the inboard pivot pylon upper skin cut-out: *DSTO F-weld test article disposition report at 29,171 SFH*, 13 February, 2007.
- [10] T V Blaricum, H Diab, M Burchill. Repair of crack in WPF upper plate FFVH 12 – Final. *DSTO F-weld test article disposition report at 24,154 SFH*, 28 September, 2006.
- [11] M Burchill, M Heller, Stress analysis of FFVH13 rework blend in F-111 A15-38. *DSTO minute, B2/129*, 21 march 2007.